

Product ion studies of diastereomeric benzo[ghi]fluoranthene-2'-deoxynucleoside adducts by electrospray ionization and quadrupole ion trap mass spectrometry

Linge Li^a, Hui-Fang Chang^b, Kenneth W. Olsen^a, Bongsup P. Cho^b, M. Paul Chiarelli^{a,*}

^a Department of Chemistry, Loyola University, Chicago, IL 60626, USA

^b Department of Biomedical Sciences, University of Rhode Island, Kingston, RI 02881, USA

Received 23 June 2005; received in revised form 8 October 2005; accepted 14 October 2005

Available online 21 November 2005

Abstract

The product ion formation characteristics of the protonated molecule ions generated from 10 different deoxynucleoside adducts of benzo[ghi]fluoranthene (B[ghi]F) have been studied using electrospray ionization (ESI) and quadrupole ion trap mass spectrometry to gain a better understanding of the fragmentation mechanisms that govern structure-specific fragmentation. The reaction of the *syn*- and *anti*-diastereomers of *trans*-3,4-dihydroxy-5,5a-tetrahydrobenzo[ghi]fluoranthene with DNA produce four deoxyguanosine, four deoxyadenosine, and two deoxycytidine adducts whose structures differ based on the *cis/trans* arrangement of the hydroxyl groups and nucleic acids bound to B[ghi]F. Those adducts that have structures where the nucleic acid and 3'-hydroxyl group of B[ghi]F are *cis* with respect to each other undergo extensive water loss whereas those isomers where the nucleic acid and 3'-hydroxyl group are *trans* do not. These results are consistent with a mechanism of water loss initiated by a hydrogen-bonding interaction between the charge-bearing proton on a heterocyclic nitrogen atom on the nucleic acid and the 3'-hydroxyl oxygen on the PAH. The dG and dC adducts are observed to undergo more extensive water loss than the dA adducts. Molecular modeling indicates that the larger relative abundances of the product ions formed by water loss for the dG and dC relative to dA are due to stronger hydrogen-bonding interactions prior to fragmentation and the greater stability of the carbocations formed at the C3' carbon after fragmentation.

© 2005 Elsevier B.V. All rights reserved.

Keywords: Electrospray ionization; Mass spectrometry; DNA adducts

1. Introduction

Interest in the analysis of carcinogen-modified nucleic acids is motivated by the belief that DNA modifications play an important role in the initiation of cancer. Polycyclic aromatic hydrocarbons (PAH) are an important class of carcinogens to which human exposure is widespread [1,2]. It is believed that PAH exert their carcinogenic effects by the metabolic oxidation of these compounds in route to DNA binding. The primary metabolic pathway involves conversion of the PAH to a diol-epoxide that binds to the primary amine groups on DNA bases [3,4].

Studies of the mutagenic potential of benzo[ghi]fluoranthene are motivated by the fact that this PAH has been detected at considerable levels in urban atmospheres and is known to have a variety of sources [5]. The rigid, planar structure of B[ghi]F suggests that it could be a good probe of the structure–activity relationships in PAH mutagenesis. This is because the diol configurations of the diastereomeric *anti*- and *syn*-diol-epoxides formed from B[ghi]F are locked into diaxial and diequatorial configurations, respectively, thus providing a means of examining the mutagenic potential of adducts that possess fixed conformations. Studies of B[ghi]F diol-epoxide diastereomers showed differences in their DNA binding *in vitro* and in the mutagenicity of the different diol-epoxide adducts when tested in *Salmonella typhimurium* TA 100 [6]. Structure–activity studies of B[ghi]F diol-epoxides *in vivo* will require analytical methodology that can differentiate the structures of benzo[ghi]fluoranthene-deoxynucleoside adducts at low levels.

* Corresponding author at: Department of Chemistry, Loyola University, 6525 N Sheridan Rd, Chicago, IL 60626, USA. Tel.: +1 773 508 3106; fax: +1 773 508 3086.

E-mail address: mchiare@luc.edu (M.P. Chiarelli).

Analytical methods based on electrospray ionization (ESI) and tandem mass spectrometry are one means of detecting bulky DNA adducts at physiologically relevant levels [7]. ESI coupled with tandem MS is used to identify and/or quantify DNA adducts in human tissue. Recent examples include the analysis of tamoxifen adducts in endometrial tissue [8], estrogen-DNA adducts in human breast tissue [9], and 4-aminobiphenyl adducts in pancreatic tissue [10]. Product ion (MS/MS) studies of carcinogen-DNA adducts derived from in vitro reactions are carried out to determine fragmentation pathways that may be used to differentiate different adduct structures when isolated from in vivo sources. Product ion analyses carried out using matrix-assisted laser desorption ionization (MALDI) and electrospray have shown promise for the differentiation of positional adduct isomers of individual nucleosides [11,12] and oligonucleotides [13,14] at low levels. Differentiating the structures of geometric isomers obtained from the reaction of a metabolized carcinogen with DNA has proven to be more challenging. However, recent studies of thymidine glycol [15], PAH-modified

nucleosides [16], and PAH-tetraols [17] suggest that diastereomers may be differentiated based on the *cis/trans* arrangement of hydroxyl groups bound to a PAH.

In this study, we examine the fragmentation characteristics of the protonated molecule ions derived from a total of 10 different B[ghi]F adducts. These adducts include four diastereomers of B[ghi]F-5a-*N*²-dG and B[ghi]F-5a-*N*⁶-dA and two diastereomers of B[ghi]F-5a-*N*⁴-dC. The ESI product ion spectra suggest that diastereomers whose structures differ based on the *cis/trans*-arrangement of the hydroxyl group and base bound to the C3' and C5a' carbons of B[ghi]F may be differentiated based on their tendency to fragment by the loss of water. Product ion formation is rationalized in terms of a mechanism that involves the formation of a hydrogen-bond between the charge-bearing proton on the nucleic acid and the C3'-oxygen on the B[ghi]F group. Molecular modeling suggests that the abundance of the fragment ions formed by water loss increases with the strength of this hydrogen-bonding interaction and the stability of benzylic carbocation formed after loss of water. This study suggests

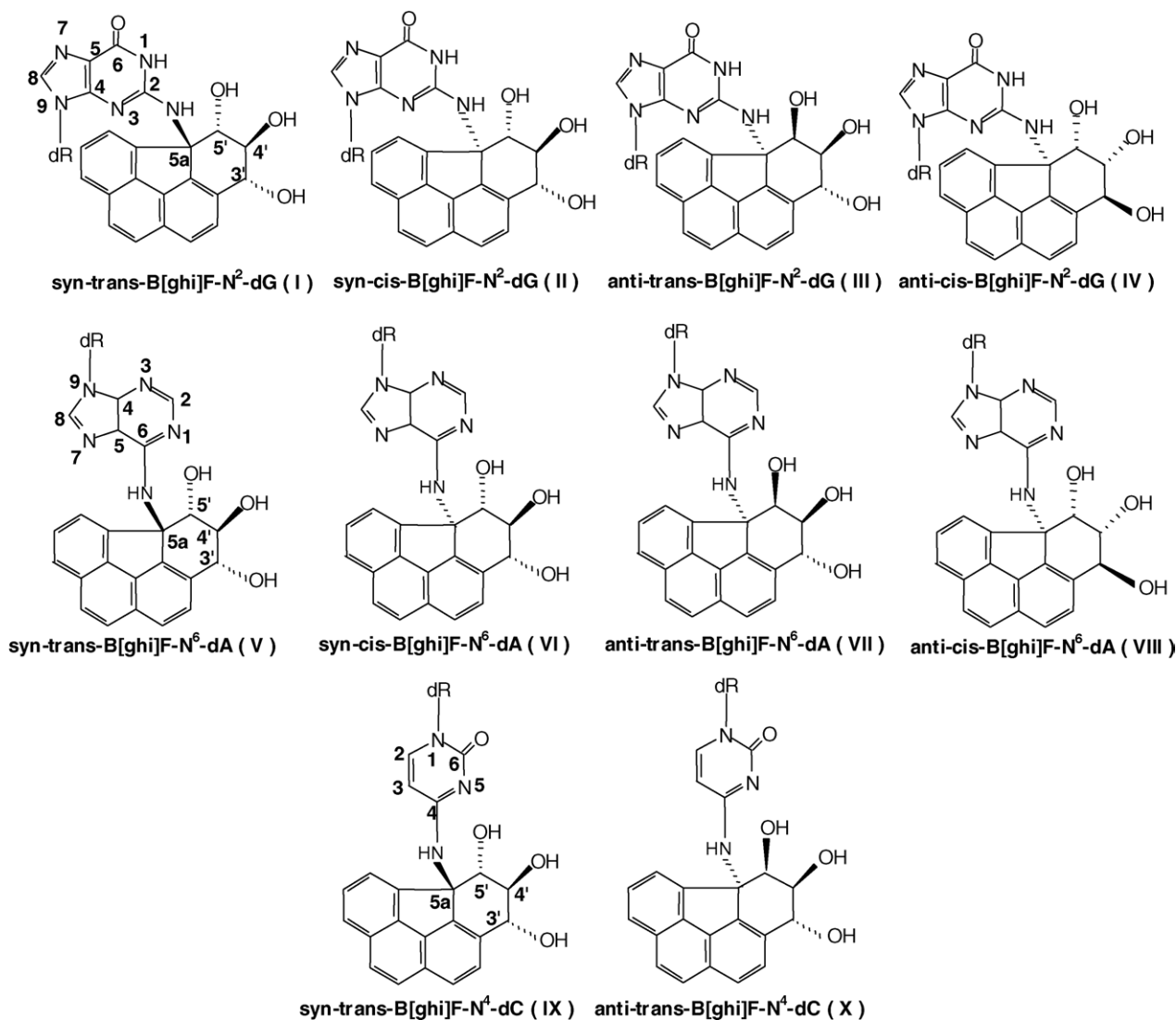


Fig. 1. The structures, and numbering of the 10 benzo[ghi]fluoranthene-deoxynucleoside adducts used in this study.

that the structures of different adduct diastereomers produced by the *syn*- or *anti*-diol-epoxide of B[ghi]F might be differentiated when DNA binding studies are carried out in rodents.

2. Experimental

2.1. Materials

2.1.1. Sample preparation

The B[ghi]F-derived deoxynucleoside adducts used in this study were synthesized by the reaction of racemic *anti*- and *syn*-B[ghi]F diol-epoxides with calf thymus DNA. The structures of these adducts are shown in Fig. 1. The structural relationship between the DNA adducts studied here and their diol-epoxide precursors is illustrated in Fig. 2. The synthesis and structural characterization of these adducts [6,18] are described elsewhere.

2.1.2. Mass spectrometry

ESI-MS and MS/MS spectra were acquired with a ThermoFinnigan Advantage (San Jose, CA) LCQ ion trap mass spectrometer. The same instrument parameter values were used for all adducts under study. The relative collision energy for MS/MS experiments was set to 35% of its maximum value for fragmentation of all the molecule ions in this study. Product ion spectra of all the BH_2^+ ions were acquired by direct infusion of low picomolar amounts of sample. A 1:1:1 mixture of water:methanol:acetonitrile was used as the mobile phase. For comparative purposes, eight product ion spectra were acquired for each compound. The capillary temperature was 200 °C and the spray voltage was 4.5 kV.

2.1.3. Molecular modeling

Molecular modeling was used to find the minimum energy conformations for the protonated nucleic acid adducts in the gas phase and the corresponding carbocations produced after the loss of water. The models were built using Spartan 5.0 (Wavefunction, Irvine, CA) and the initial geometry was optimized using the PM3 semi-empirical method as implemented in Spartan. Models were constructed for the adenine, guanine and cytosine adducts of B[ghi]F. Calculations were carried out assuming that charge-bearing proton was attached to a nitrogen atom of the base ring. Starting with this optimized structure for each protonated adduct, a conformational search was done rotating about the two conformational sensitive bonds on either side of the nitrogen bridging the base and the PAH. The 36 conformations generated for each structure were geometry optimized using PM3 and the final energies were compared. Additional starting structures were generated by constraining the NH to O distance of a potential hydrogen bond to 2 Å and then initially minimizing the energy of the structure using a molecular mechanics potential function. These structures were also geometry optimized using PM3 and the final energies were compared with those obtained earlier via the conformational search. Vibrational frequencies computed for the optimized structures were universally positive, indicating that the geometries were positioned at energy minima. The results were similar for both methods since the final energies were calculated using PM3, but the combination of these methods gave a complete picture of conformational space for all adducts. The carbocation structures were generated by maintaining the most stable adduct conformations after removing water. Single point energies were calculated using the PM3 method for each carbocation for comparison.

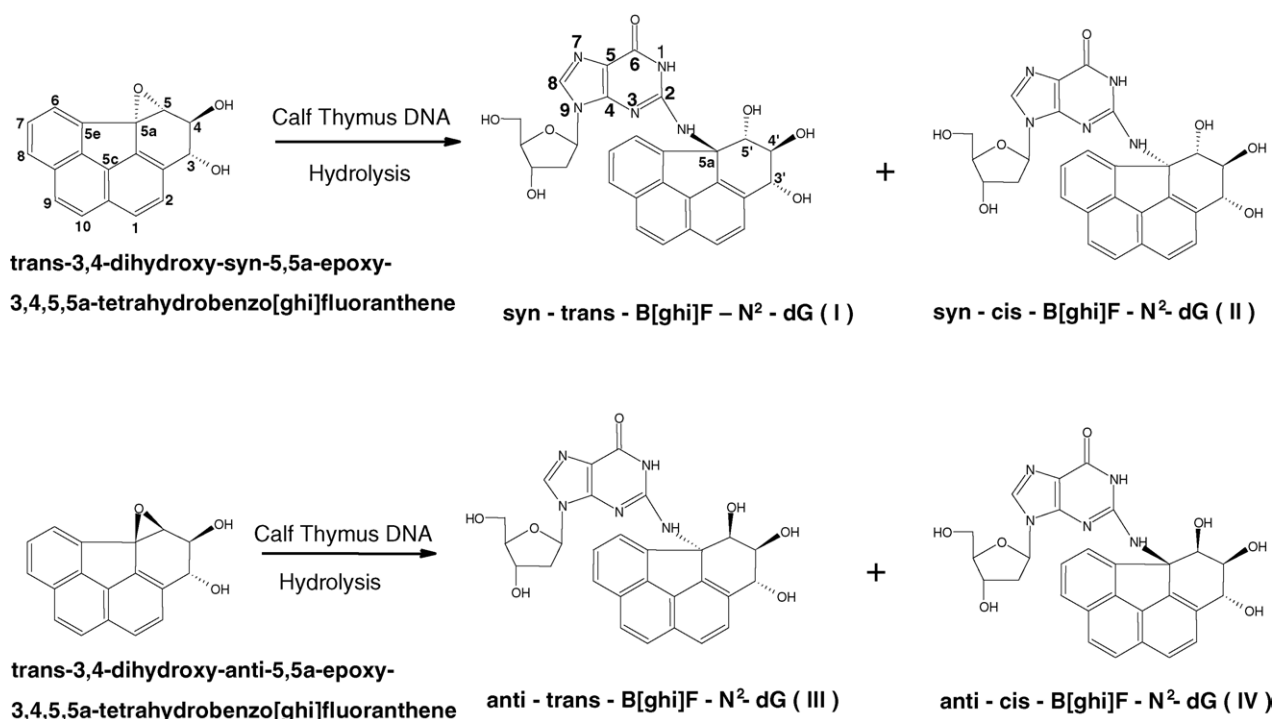


Fig. 2. The structures of the B[ghi]F-dG adducts formed by the reaction of DNA with the diol-epoxide diastereomers *trans*-3,4-dihydroxy (*anti*)- and *trans*-3,4-dihydroxy (*syn*)-5,5a-epoxy-3,4,5,5a-tetrahydrobenzo[ghi]fluoranthene.

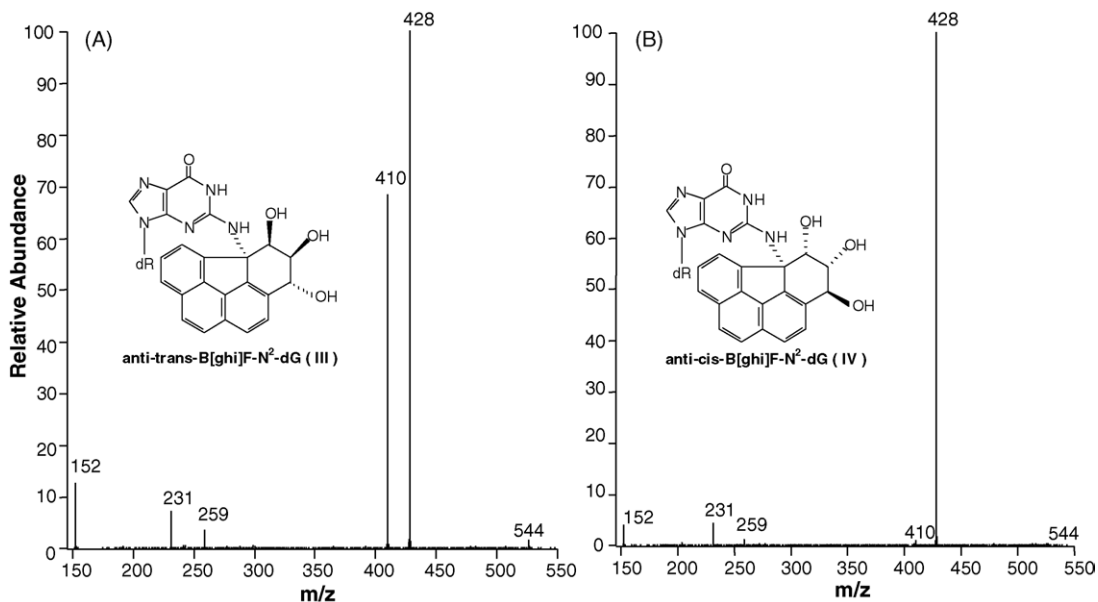


Fig. 3. ESI/QIT product ion mass spectra of the $[M + H]^+$ ion at m/z 544 formed from (A) *anti-trans*-B[ghi]F-N²-dG (III) and (B) *anti-cis*-B[ghi]F-N²-dG (IV).

3. Results and discussion

3.1. Fragmentation characteristics of B[ghi]F adducts

Motivation for the product ion studies of these ten B[ghi]F deoxynucleoside adducts is two-fold. The first is to determine fragmentation pathways that may be used to differentiate the structures of different diastereomeric adducts. The second is to gain a better understanding of the fragmentation mechanism(s) that govern this structure-specific fragmentation through the comparison of product ion spectra of the protonated molecule

ions acquired from B[ghi]F adducts of different deoxynucleosides. MALDI-PSD studies of the four dA-N⁶-B[ghi]F adducts indicate that water loss is favored for those adducts where the 3'-hydroxy group of B[ghi]F and the nucleic acid are *cis* with respect to each other. However, comparison of the PSD spectra acquired using the dA adducts with B[ghi]F adducts of dG and dC was not possible because the dG and dC adducts did not yield $(M + H)^+$ ions of sufficient abundance for the acquisition of PSD spectra [16].

The fragmentation pathway that is most indicative of structural differences between these diastereomeric B[ghi]F adducts

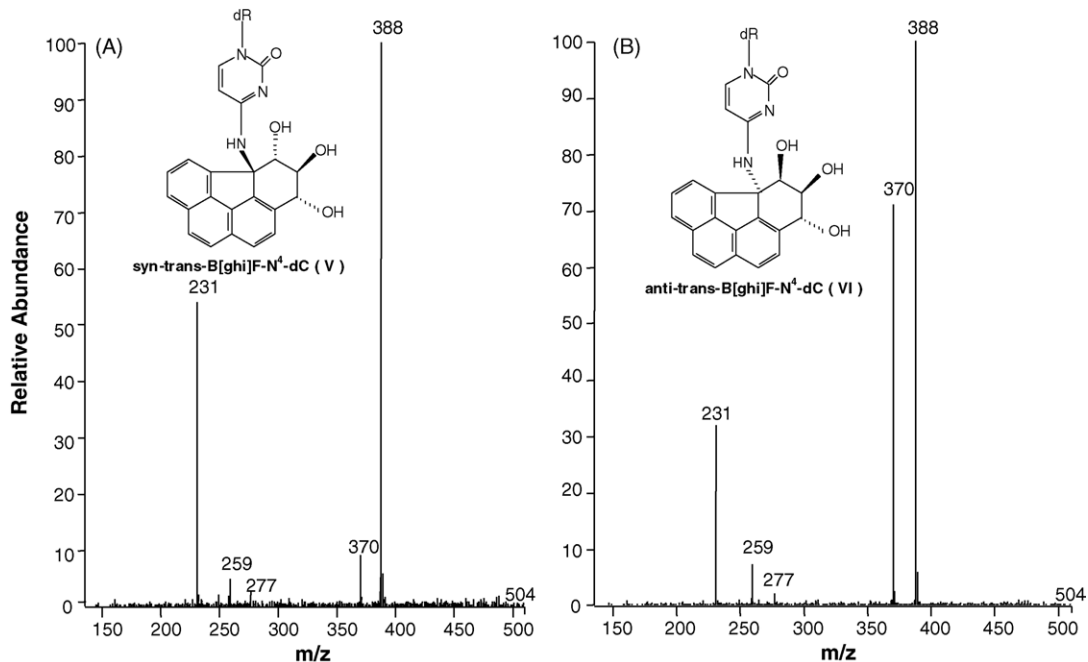


Fig. 4. ESI/QIT product ion mass spectra of the $[M + H]^+$ ion at m/z 528 formed from (A) *anti-trans*-B[ghi]F-N⁶-dA (VII) and (B) *anti-cis*-B[ghi]F-N⁶-dA (VIII).

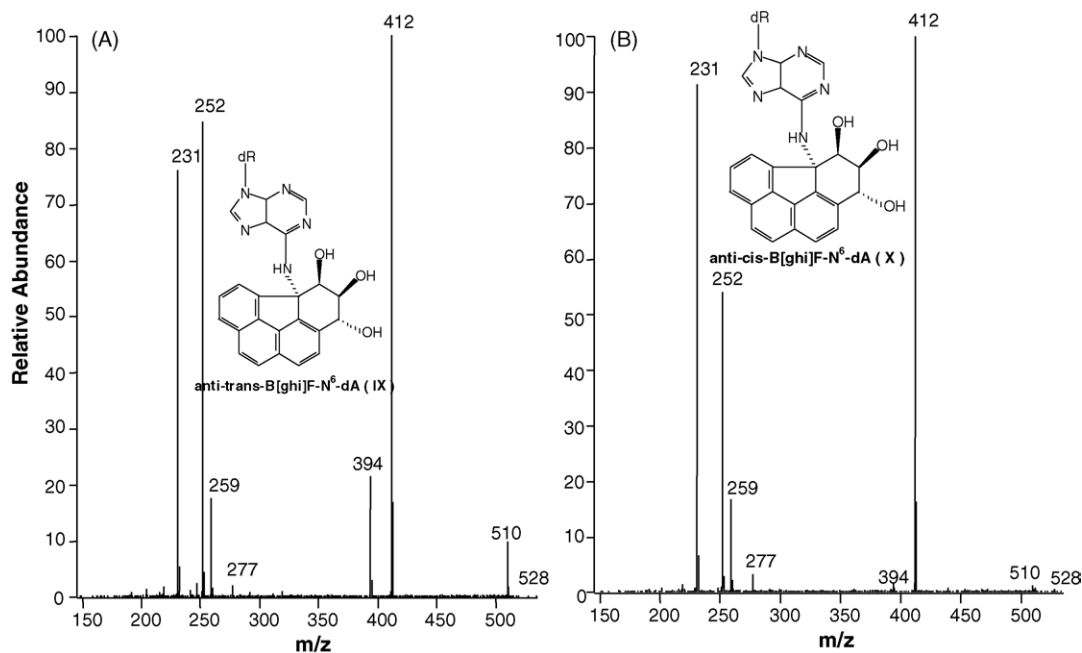


Fig. 5. ESI/QIT product ion mass spectra of the $[M+H]^+$ ion at m/z 504 formed from (A) *syn-trans*-B[ghi]F- N^6 -dC (IX) and (B) *anti-cis*-B[ghi]F- N^6 -dC (X).

is loss of water from the BH_2^+ ion after the loss of the deoxyribose. Those adducts where the nucleic acid and 3'-hydroxy group on the B[ghi]F are *cis* with respect to each other show a much greater propensity to undergo water loss than those adducts where these two functional groups are *trans* with respect to each other. This difference in water loss abundance is most pronounced for the *cis/trans* isomers of dG and dC. Representative product ion spectra of all the B[ghi]F adducts used in this study are shown in Figs. 3–5. The most abundant fragment ions observed in all spectra are formed by the loss of the deoxyribose group. The m/z values associated with the fragment ions formed by consecutive losses of the deoxyribose and water are m/z 410 (dG, Fig. 3), m/z 370 (dC, Fig. 4), and m/z 394 (dA, Fig. 5). The other fragmentation pathways observed here are consistent with those described previously [19,20] and do not appear to be indicative of the geometric isomerism of these compounds. The average relative abundances of all product ions observed in these determinations are summarized in Table 1. The ions at m/z 277, 259, and 231 are formed from bond cleavages in the trihydroxy B[ghi]F group.

3.2. Mechanism of water loss

The relative abundances of the fragment ions in Table 1 suggests a mechanism of water loss that proceeds from a precursor ion conformation that possesses a hydrogen bond between a protonated nitrogen on the nucleic acid and the 3'-oxygen on the B[ghi]F group, as was suggested previously in MALDI-PSD studies of the four deoxyadenosine adducts [16]. Molecular modeling was carried out to explain the differences in the relative abundances of the $BH_2^+-H_2O$ ions observed in the ESI product ion spectra of the five adducts observed to undergo extensive water loss. The mechanism of water loss suggested by the observed fragmentation is shown in Fig. 6 for *anti-trans*-dC- N^4 -

B[ghi]F. Water loss is preceded by the formation of a hydrogen bond between the charge-bearing proton attached to nitrogen in the six-membered pyrimidine ring and the 3'-hydroxyl oxygen on the B[ghi]F ring. After collisional activation, cleavage of

Table 1

Average relative abundances of the product ions formed in CAD of the protonated molecule ions derived from the B[ghi]F adducts used in this study

2'-Deoxyguanosine- N^2 -benzo[ghi]fluoranthene adducts				
m/z	<i>syn-trans</i> (I)	<i>syn-cis</i> (II)	<i>anti-trans</i> (III)	<i>anti-cis</i> (IV)
428	100	100	100	100
410	1.1 ± 0.2	17.7 ± 0.7	70 ± 2	1.6 ± 0.4
277	0.4 ± 0.1	0.2 ± 0.1	0.6 ± 0.2	0.4 ± 0.2
259	1.1 ± 0.2	0.9 ± 0.2	3.8 ± 0.4	1.2 ± 0.2
231	4.4 ± 0.2	4.9 ± 0.3	6.3 ± 0.6	9.4 ± 0.6
152	4.0 ± 0.3	7.8 ± 0.2	14 ± 1	7.8 ± 0.6
2'-Deoxyadenosine- N^6 -benzo[ghi]fluoranthene adducts				
m/z	<i>syn-trans</i> (V)	<i>syn-cis</i> (VI)	<i>anti-trans</i> (VII)	<i>anti-cis</i> (VIII)
510	4.5 ± 0.4	1.1 ± 0.3	10 ± 1	1.6 ± 0.5
412	64 ± 3	43 ± 3	100	99 ± 1
394	6.7 ± 0.5	0.9 ± 0.3	22 ± 1	1.9 ± 0.4
277	1.7 ± 0.3	0.9 ± 0.2	2.5 ± 0.6	3.0 ± 0.5
259	8.7 ± 0.9	4.7 ± 0.5	18 ± 1	17 ± 1
252	66 ± 3	100	84 ± 3	61 ± 3
231	100	45 ± 2	81 ± 4	97 ± 2
2'-Deoxycytidine- N^4 -benzo[ghi]fluoranthene adducts				
m/z	<i>syn-trans</i> (IX)	<i>anti-cis</i> (X)		
388	100	100		
370	6 ± 2	73 ± 5		
277	2.3 ± 0.2	2.5 ± 0.4		
259	4.9 ± 0.5	7.4 ± 0.7		
231	54 ± 3	32 ± 2		

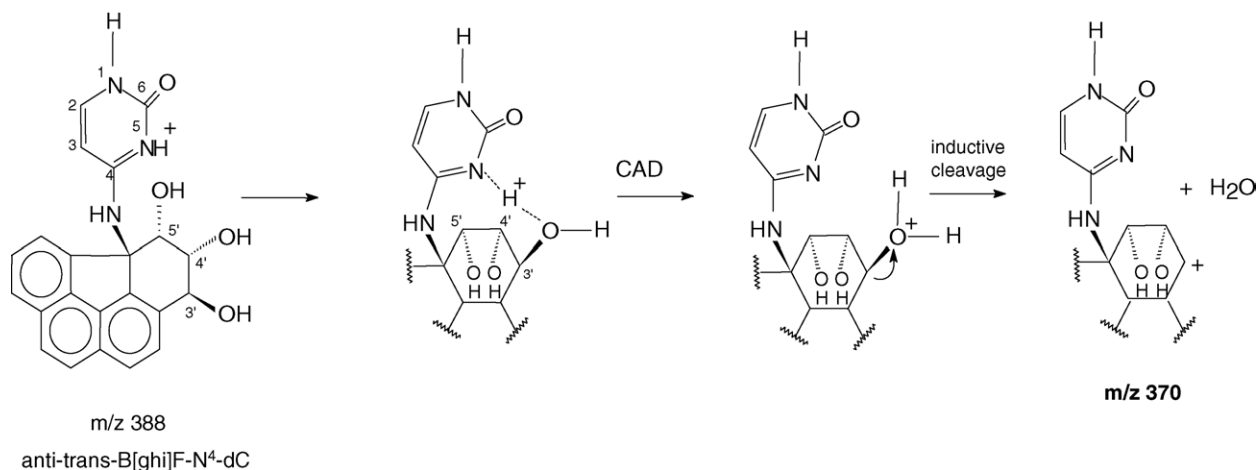


Fig. 6. Proposed mechanism of water loss from the BH₂⁺ ion formed from *anti-trans*-B[ghi]F-dC (X).

the C3'–O3' bond produces a carbocation localized at the C3' position of the B[ghi]F group.

3.3. Molecular modeling

We carried out semiempirical molecular modeling of the protonated-adduct molecular ions to determine if hydrogen-bonding interactions between the base and B[ghi]F hydroxyl oxygens were possible. The heats of formation of different carbocations formed by water loss were calculated as well to identify the most stable fragment ion structures. The results of these calculations are summarized in Table 2. These calculations suggest several aspects of the fragmentation mechanism and they are summarized as follows.

Stable hydrogen bonds (less than 3 Å in length) are only possible when the base and the hydrogen-acceptor oxygen

must be on the same side of the PAH ring. Examination of Table 1 shows that all cases where no hydrogen bond could be found the base nitrogen and B[ghi]F hydroxyl oxygens were *trans* with respect to each other. The hydrogen bonds formed for *cis*-cytosine adducts are more stable ($\Delta H_f = 94$ kcal/mol) than those formed by guanosine ($\Delta H_f = 115$ kcal/mol) or adenosine ($\Delta H_f = 165$ kcal/mol). The position of the hydroxyl group did not significantly affect the stability of the hydrogen-bonded structures. The average ΔH_f 's for these structures were 134 kcal/mol for adducts involving hydrogen bonds to the 3'O, 139 kcal/mol for adducts involving hydrogen bonds to the 4'O and 133 kcal/mol for adducts involving hydrogen bonds to the 5'O.

Carbocations formed after the elimination of water were slightly more stable for cytosine adducts than for adenine or guanine adducts. The average ΔH_f 's for these carbocation struc-

Table 2
Calculated heats of formation (kcal/mol) for the hydrogen-bonded intermediates and carbocations formed during the fragmentation of the protonated molecule ions derived from the 2'-deoxynucleoside-B[ghi]F adducts in this study

Adduct	NH ⁺	5'O		4'O		3'O	
		H-bond	Carbocation	H-bond	Carbocation	H-bond	Carbocation
<i>syn-trans</i> -B[ghi]F-N ² -dG (I)	1	nf		122	292	nf	
	3	nf		118	274	nf	
<i>syn-cis</i> -B[ghi]F-N ² -dG (II)	1	105	273	nf		105	251
	3	116	274	nf		118	251
<i>anti-trans</i> -B[ghi]F-N ² -dG (III)	1	nf		nf		109	251
	3	nf		nf		116	251
<i>anti-cis</i> -B[ghi]F-N ² -dG (IV)	1	118	288	120	287	nf	
	3	116	277	120	280	nf	
<i>syn-trans</i> -B[ghi]F-N ⁶ -dA (V)	1	nf		164	319	nf	
	7	nf		165	323	nf	
<i>syn-cis</i> -B[ghi]F-N ⁶ -dA (VI)	1	158	316	nf		160	292
	7	172	319	nf		160	291
<i>anti-trans</i> -B[ghi]F-N ⁶ -dA (VII)	1	nf		nf		173	299
	7	nf		nf		167	295
<i>anti-cis</i> -B[ghi]F-N ⁶ -dA (VIII)	1	159	321	166	325	nf	
	7	165	318	168	324	nf	
<i>syn-trans</i> -B[ghi]F-N ⁴ -dC (IX)	5	nf		92	251	nf	
<i>anti-trans</i> -B[ghi]F-N ⁴ -dC (X)	5	nf		nf		98	233

nf: not formed.

tures were 261 kcal/mol for the adenine adducts, 270 kcal/mol for guanine adducts and 246 kcal/mol for cytosine adducts. Carbocations formed after the elimination of water were more stable when the 3'-hydroxyl group was eliminated than when the 4'- or 5'-hydroxyl groups were removed. The average ΔH_f s for these carbocation structures were 270 kcal/mol for adducts involving hydrogen bonds to the 3'O, 297 kcal/mol for adducts involving hydrogen bonds to the 4'O and 293 kcal/mol for adducts involving hydrogen bonds to the 5'O. As we have previously observed [16] the carbocation formation at the B[ghi]F-C3' benzylic carbon (after loss of the protonated hydroxyl group) is favored over carbocation formation at the C4' or C5' positions of the B[ghi]F by ca. 25 kcal/mol. Therefore, inductive cleavage of the C3'-O3' bond should proceed more readily than the cleavage of the C4'-O4' or C5'-O5' bonds. Two of the five adducts that undergo water loss (*syn-cis* adducts **II** and **VI**) are capable of forming O5' as well as O3' hydrogen bonds. The relative abundances of water loss ions are less for the *syn-cis* adducts than for the three *anti-trans* adducts (**III**, **VII**, and **X**) that form only O3' hydrogen bonds. These observations suggest that formation of the O5' hydrogen bond decreases the water loss fragmentation pathway. The results of these calculations support the mechanism of water loss proposed in Fig. 6.

4. Conclusion

The product ion formation characteristics of 10 benzo[ghi]fluoranthene-deoxynucleoside adducts have been studied by electrospray ionization and ion trap MS to determine fragmentation pathways that may be used to differentiate the structures of these adducts when detected in vivo. The reaction of each diol-epoxide produces two adducts that differ in structure based on the *cis/trans* arrangement of the hydroxyl group and the nucleic acid bound to the C3' and C5a' carbons of B[ghi]F. The relative abundance of the water loss ions observed in the product ion spectra are greatest for the dC and dG adducts and those adducts that have an *anti-trans* configuration. These structural features are consistent with a mechanism of water loss that is initiated by a hydrogen-bonding interaction between the charge-bearing proton on the nucleic acid nitrogen and the 3'-hydroxyl oxygen on the B[ghi]F group. The results of this study suggest that the structures and quantities of individual

B[ghi]F-DNA adduct diastereomers may be determined in a rodent model when a single B[ghi]F diol-epoxide is studied.

Acknowledgement

This work was supported in part by a grant (to MPC) from the American Cancer Society (RPG-00-233-01-CNE).

References

- [1] R.G. Harvey, Polycyclic Aromat. Compd. 9 (1996) 1.
- [2] IARC. IARC Monographs on the Evaluation of the Carcinogenic Risk of Chemicals to Humans, vol. 38. IARC Publishers, Lyon, France, 1986.
- [3] A. Dipple, Q.A. Khan, J.E. Page, I. Ponten, J. Szeliga, Int. J. Oncol. 14 (1999) 103.
- [4] F.A. Beland, M.C. Poirier, in: A.E. Sirica (Ed.), The Pathobiology of Neoplasia, Plenum Press, New York, 1989, p. 57.
- [5] R.G. Harvey, Polycyclic Aromatic Hydrocarbons: Chemistry and Carcinogenicity, Cambridge University Press, Cambridge, UK, 1991.
- [6] H.-F. Chang, D.M. Huffer, M.P. Chiarelli, L.R. Blankenship, S.J. Culp, B.P. Cho, Chem. Res. Toxicol. 15 (2002) 198.
- [7] J.H. Banoub, R.P. Newton, E. Esmans, D.F. Ewing, G. Mackenzie, Chem. Rev. 105 (2005) 1869.
- [8] F.A. Beland, M.I. Churchwell, D.R. Doerge, D.R. Parkin, D. Malejka-Giganti, A. Hewer, D.H. Philips, P.L. Carmichael, G.G. da Costa, M.M. Marques, J. Natl. Cancer Inst. 96 (2004) 1099.
- [9] J. Embrechts, F. Lemiere, W. Van Dongen, E.L. Esmans, P. Buyaert, E. Van Marck, M. Kockx, A. Makar, J. Am. Soc. Mass Spectrom. 14 (2003) 482.
- [10] E.M. Ricicki, J.R. Soglia, C. Teitel, R. Kane, F. Kadlubar, P. Vouros, Chem. Res. Toxicol. 18 (2005) 692.
- [11] J. Embrechts, F. Lemiere, W. Van Dongen, E.L. Esmans, J. Mass Spectrom. 36 (2001) 317.
- [12] L. Li, M.P. Chiarelli, P.S. Branco, A.M. Antunes, M.M. Marques, L.L. Goncalves, F.A. Beland, J. Am. Soc. Mass Spectrom. 14 (2003) 1488.
- [13] R. Song, W. Zhang, H. Chen, H. Ma, Y. Dong, G. Sheng, Z. Zhen, J. Fu, Rapid Commun. Mass Spectrom. 19 (2005) 1120.
- [14] Y. Wang, J.-S. Taylor, M.L. Gross, J. Am. Soc. Mass Spectrom. 12 (2001) 1174.
- [15] Y. Wang, S. Vivekananda, K. Zhang, Anal. Chem. 74 (2002) 4505.
- [16] M.P. Chiarelli, H.-F. Chang, K.W. Olsen, D. Barbacci, B.P. Cho, D.M. Huffer, Chem. Res. Toxicol. 16 (2003) 1236.
- [17] D.M. Huffer, H.-F. Chang, B.P. Cho, L. Zhang, M.P. Chiarelli, J. Am. Soc. Mass Spectrom. 12 (2001) 376.
- [18] H.-F. Chang, D.M. Huffer, M.P. Chiarelli, B.P. Cho, Chem. Res. Toxicol. 15 (2002) 187.
- [19] P.S. Branco, M.P. Chiarelli, J.O. Lay Jr., F.A. Beland, J. Am. Soc. Mass Spectrom. 6 (1995) 248.
- [20] E.A. Stemmler, M.V. Buchanan, G.B. Hurst, R.L. Hettich, Anal. Chem. 66 (1994) 1274.